Interfacial Dissociation and Unfolding of Glucose Oxidase

Jian R. Lu* and Tsueu-Ju Su

Department of Physics, UMIST, P.O. Box 88, Manchester M60 1QD, United Kingdom

Dimitra Georganopoulou and David E. Williams

Department of Chemistry, University College London, London, 20 Gordon St, London WC1H 0AJ, United Kingdom

Received: October 17, 2002; In Final Form: February 13, 2003

The effect of solution ionic strength on the dissociation and unfolding of glucose oxidase (GOx) adsorbed at the air/water interface has been studied by specular neutron reflection. The structure and composition of the GOx layers was determined at pH 7 under null reflecting water (NRW) comprised of D_2O and H_2O with a molar ratio close to 1:11. Under this isotopic contrast, the specular reflectivity arises entirely from the adsorbed layer. At the lower ionic strength of 4.5 mM, GOx adsorption forms a uniform layer of some 30 Å thick. The layer thickness tends to increase with bulk GOx concentration and eventually reaches the short axial length of the enzyme's globular monomer structure of 37 Å. These results suggest that while the enzyme is dissociated into monomers it does not unfold further into the distributions characteristic of random polypeptide segments. At the higher ionic strength of 0.45 M, the thickness of the GOx layers is between 40 and 50 Å when the bulk GOx concentration is below 0.4 μM. This dimension is close to the short axial length of the globular dimer of 52 Å, suggesting that at the higher ionic strength the enzyme adsorbs with its long 80 Å axis parallel to the surface of water. As the concentration is increased above 1 μM, a secondary layer starts to form on the solution side of the main surface layer, leading to a bilayer adsorption of some 50 Å for each layer. Although the inner solution layer only contains some 5−8% of the adsorbed material, neutron reflection is sufficiently accurate to detect its structural dimension. Further neutron measurements under D_2O suggest that the dissociated monomers and the dimers have different extent of immersion into the aqueous subphase. This observation is consistent with the different surface activities of the two species, which are related to the distributions of amino acid groups on their outer surfaces.

Introduction

Proteins and enzymes contain hydrophilic and hydrophobic domains, most of which form well defined three-dimensional structures. The stability of their globular framework may vary when the protein chains are subject to single mutations or under delicate changes of physicochemical conditions. Protein folding, unfolding and aggregation have recently attracted a wide range of interest both fundamentally and from biotechnological applications. In particular, recent studies have indicated that protein unfolding and misfolding may have direct implications in the causation of diseases.[1−3]

Current characterization of protein structural misfolding and aggregation has been mainly performed with the protein in a bulk solution environment. In contrast, the majority of biological events involving proteins and enzymes occur across cell membranes and biointerfaces. Interfacial processes represent different energetic balances and a different physicochemical environment, and will have different implications for the structural stability and enzymatic activity. The aim of this work is to demonstrate how interfacial adsorption affects structural unfolding of glycoproteins under a set of controlled surface and solution conditions. Glucose oxidase (GOx) is chosen as the model glycoprotein in this study because its interfacial activity at the molecular level underpins a diverse range of technological applications. GOx adsorption has been extensively studied with the aim of achieving efficient design of artificial systems such as biosensors.[4−6] There is also strong impetus to improve the enzymatic performance and biostability of GOx in biocatalysis on supported substrates. The air/water interface represents the simplest model that allows the assessment of the effect of hydrophobic and hydrophilic polarization to be made upon biomolecular surface assembly.

Upon adsorption, the polarized nature of the interface may drive glycoproteins such as GOx to unfold, resulting in irreversible surface aggregation and precipitation. Various techniques have been used to investigate the dynamic and equilibrium process of protein layers adsorbed at interfaces. Surface tension measurements[7,8] have been most widely used to follow the changes of protein adsorption with time and solution concentration, but because the interfacial process is rather complex and in many cases the systems deviate heavily from ideal solution behavior, little reliable information can be extracted about the molecular events involved. Radiolabeling offers some direct estimate of the adsorbed amount,[9−10] but this technique does not allow the conformational structure within the adsorbed layer to be probed. In many cases, the attachment of radioactive fragments may alter surface activity of the biomolecules concerned. Techniques such as X-ray reflection and ellipsometry determine the variations of the total electron density and refractive index profile perpendicular to the interface, but their inability in distinguishing water from the

* Corresponding author. Phone: 44-161-2003926. E-mail: j.lu@umist.ac.uk.

10.1021/jp0272320 CCC: $25.00
Published on Web 04/01/2003

adsorbed molecules means that these techniques can at most assess the relative adsorbed amount. It is, however, interesting to note that second-harmonic generation[11] (SHG) has recently emerged as a new technique to probe structural reorientation of GOx adsorbed at the surface of water.

Neutron reflection on the other hand is a very sensitive and accurate technique that has also been developed for the study of a range of interfacial processes involving proteins.[12−15] The high resolution of neutron reflectivity allows a reliable determination of protein layer density distribution along the surface normal direction. Therefore, accurate measurements of the adsorbed amount, as well as its layer thickness determined with a few Å resolution, in conjunction with the known dimension of the globular structure, can provide information about the physical state of the protein within the adsorbed layer. The use of D_2O as a solvent allows the determination of the extent of mixing of the layer with water, and its protrusion to air.

In this study we demonstrate the use of neutron reflection for the determination of unfolding of the globular structure of glucose oxidase at an interface, influenced by the salt concentration. GOx is a dimeric globular glycoprotein[16] of dimensions $60 \times 52 \times 77$ Å^3, made up from two identical subunits (monomers), each of molecular weight ca. 77 000 Da and of dimension $60 \times 52 \times 37$ Å^3. The two subunits are tightly bound noncovalently with ion bridges and hydrogen bonds. Sun et al.[17] have recently shown that the observed surface area per enzyme molecule varied from 700 to 2200 Å^2, for the enzyme layer spread on the surface of water, whereas Fiol et al.,[18] on the basis of the dimensions given above (Hecht et al.[16]), have estimated an area for the dimer of some 4000 Å^2. The mean diameter in solution of the native enzyme, determined by photon correlation spectroscopy, is some 76 Å at pH 7.4.[19] This compares well with the Stokes radius of ca. 43 Å with a frictional ratio of 1.21 obtained by the same group of authors. These results confirm that under aqueous solution conditions the enzyme is an elongated protein with rigid structure and its dimensions are comparable to a compact spheroid of $60 \times 52 \times 77$ Å^3 as in its crystalline form. Although GOx retains its globular structure in aqueous solution (e.g., see ref 19), structural deformation may occur upon interfacial adsorption because a number of additional factors affect the globular stability. For the adsorption at the air/water interface, which is the simplest interface to study, the interfacial anisotropy generates powerful forces which might make the structure of the GOx adsorbed on the surface quite different from that in the bulk. The surface induces hydrophobic/hydrophilic polarization, which will realign various amino acid residues and will tend to unravel the secondary and tertiary structures of the protein. It is generally perceived that proteins exhibit their surface activity mainly as a result of uneven distributions of polar, nonpolar, and charged groups on the surfaces of protein molecules. The surface adsorption will promote segregation, resulting in the preferential exposure of hydrophobic parts in air and polar and charged groups in water. Any loss of tertiary structure would be characterized by inhomogeneous peptide density distributions along the surface normal and this structural feature can be easily probed by neutron reflection.

The present work reports neutron reflection from GOx layers adsorbed at the aqueous solution−air interface. The resultant sensitive determination of surface layer thickness and composition has revealed that adsorbed GOx is dissociated into monomers at the lower salt concentration, but that the dimeric globular structure is retained at the higher salt concentration. Moreover, the accurate determination of layer thickness and surface excess suggests a substantial structural deformation for both dimers and monomers, although such deformation does not lead to their complete breakdown into polypeptides.

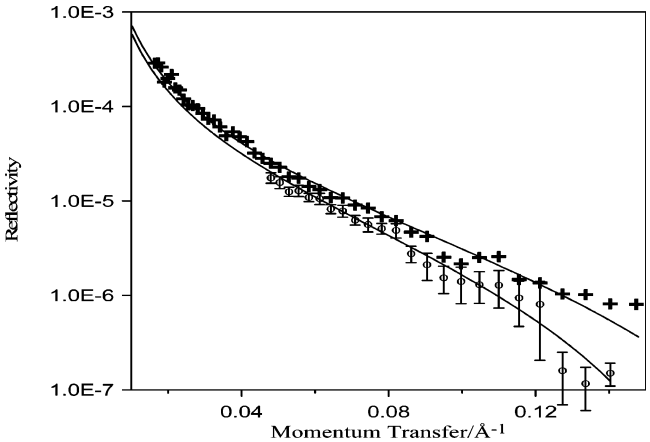

Figure 1. Neutron reflectivity measured after 1 h (○) and 12 h (+) of placement of 0.1 μM GOx solution in Teflon trough. The ionic strength of the solution was fixed at 4.5 mM using phosphate buffer.

Results

In the following we will first show the neutron measurements on NRW, which offer information about the variation of GOx surface adsorbed amount (surface excess) with bulk concentration and the effect of total ionic strength (controlled by varying the concentration of phosphate buffer). The extent of immersion of GOx layer into aqueous subphase is determined from the reflectivity profiles measured under D_2O. These neutron reflection data present an overview of the main structural features of GOx layers adsorbed on the surface of water.

A. GOx Dynamic Adsorption. The kinetic features of GOx adsorption were first characterized using surface tension measurements. This preliminary study helped to obtain the main experimental conditions for the neutron experiment. The surface tension was found to take hours to reach stable readings. As found for most other proteins, the lower the GOx concentration, the longer the equilibration process. The time scale to reach stable surface tension readings varied from a few hours to some 14 h. The time-dependent adsorption of GOx could also be followed directly by neutron reflection. Figure 1 shows the example of two reflectivity profiles measured after 1 and 10 h equilibration from a solution containing 0.1 μM GOx buffered at pH 7. The ionic strength was set at approximately 4.5 mM using phosphate buffer. The reflectivity is plotted as function of momentum transfer, κ, perpendicular to the reflecting surface where

$$\kappa = \frac{4\pi \sin \theta}{\lambda} \tag{1}$$

where θ is the incidence angle and λ the wavelength of the incidence neutron beam. The aqueous solution used was NRW water, and as already indicated, the specular reflectivity under NRW was entirely from the adsorbed GOx layer because the solvent was made invisible to neutrons. Each of the reflectivity profiles was run for about 1 h for a sufficiently good statistical quality. Two main observations can immediately be made from Figure 1. First, the level of reflectivity increases with time, indicating a trend of increasing surface excess as the layer is aged. Second, the reflectivity profile becomes less tilted with time, signifying a decrease of average layer thickness. The

results thus suggest that as the GOx layer tends to equilibrium adsorption, its thickness drops and the layer gets denser.

Quantitative data analysis using the optical matrix method has been used to derive structural parameters from the measured reflectivity profiles. The data were well fitted by the uniform layer model. The calculated reflectivity profiles are shown as continuous lines in Figure 1. The uniform layer model fitting leads directly to layer thickness (τ) and scattering length density (ρ), from which the area per molecule (A) and surface excess (Γ) can be calculated using the following two equations:[20,21]

$$A = \frac{\sum m_p b_p}{\rho \tau} \tag{2}$$

where $\sum m_p b_p$ is the total scattering length for protein. The surface excess is then calculated by

$$\Gamma = \frac{\mathrm{MW}}{6.02 \times A} \tag{3}$$

where MW is the protein molecular weight. The analysis showed that after 1 h adsorption the GOx layer was 40 ± 3 Å thick and A was 17 600±2000 Å^2, corresponding to a value of Γ of 9.5 × 10^{-9} mol m^{-2}. After 10 h equilibration, τ = 28 ±3 Å, A = 15 700 ± 2000 Å^2, and $\Gamma = 1.1 \times 10^{-8}$ mol m^{-2}.

The reflectivity profile after 1 h adsorption was measured only at a beam incidence angle of 1.5°. It can be seen from Figure 1 that the specular signal mainly occurs over the κ range below 0.1 Å^{-1}, above which the reflectivity falls into the constant background. It would thus appear to be more sensible to perform the dynamic scan at a lower beam incidence angle, but this was prohibited by the inaccurate calibration D_2O run. On reflectometer Surf the calibration could only be made against D_2O measured at 1.5°. After the adsorption had been equilibrated, reflectivity profiles measured at the lower beam incidence angles of 0.8° and 0.5° could reliably be merged with the corresponding profile measured at 1.5° and hence calibrated against D_2O. It can be seen from Figure 1 that the reflectivity measured at 1.5° after 1 h adsorption provides sufficient evidence of time dependent adsorption when compared with the measurement obtained over the wider κ range obtained after 10 h adsorption.

B. Structure Dissociation at Low Salt Concentration. Neutron reflectivity was measured over a range of GOx concentration in order to assess the progressive structural change of GOx layers at the interface. The total ionic strength in these measurements was all controlled at 4.5 mM. The reflectivity profiles shown in Figure 2 are plotted against log κ so that the differences between them are better displayed. Figure 2 shows that the level of reflectivity initially increased rapidly with increasing concentration but above 0.1 μM further increase in concentration resulted in a much reduced increment in surface excess, indicating that the system was approaching saturated adsorption. Moreover, the reflectivity profiles shown in Figure 2 are, within the experimental error, parallel to each other, indicating that although the surface excess increased steadily the thickness of the GOx layer did not vary significantly.

Quantitative structural information was obtained from model fitting, and the continuous lines shown in Figure 2 were calculated assuming that the adsorbed enzyme layer followed a uniform layer distribution. It can be seen from Figure 2 that the calculated curves fit the measured reflectivity well below 0.1 Å^{-1}. At κ > 0.1 Å^{-1}, the signal was weak, and the data were compromised by the high level of incoherent background.

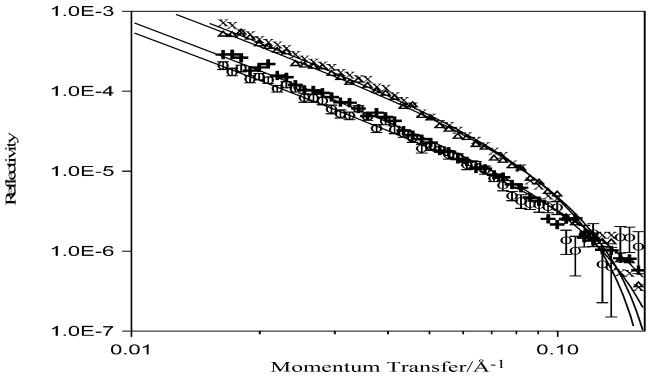

Figure 2. Neutron reflectivity measured from equilibrated GOx solution surfaces at the bulk concentrations of 0.01 (○), 0.1 (+), 0.4 (△) and 1 μM (×). The total ionic strength was fixed at 4.5 mM. The continuous lines represent uniform layer model fits with GOx layer thickness varying from 25 to 37 Å, indicating sideways on monomer adsorption.

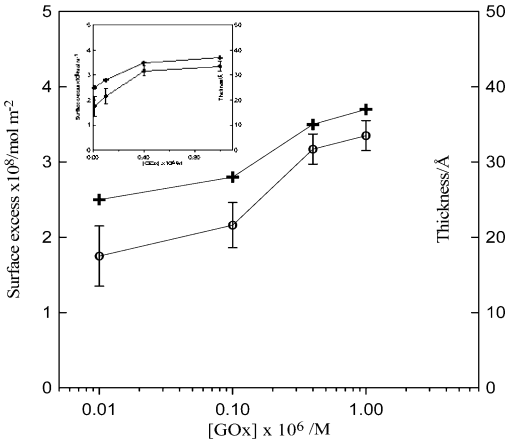

Figure 3. Variation of GOx surface excess (○) and layer thickness (+) with bulk GOx concentration. The total solution ionic strength was fixed at 4.5 mM. The plots of the two parameters against the linear GOx concentration are also inserted for comparison.

The increasing extent of uncertainty of the measured data at high κ is also evident from the greater error bars (shown only for one set of reflectivity profile for clarity). The data analysis leads to the simultaneous determination of surface excess and layer thickness, and the resulting parameters obtained are shown in Figure 3. At the lowest GOx concentration of 0.01 μM the layer was 25 ± 2 Å thick, with an area per molecule of some 17 000 Å^2. This layer thickness may suggest that under these solution conditions the enzyme may adsorb in the form of monomers. Because the short axial length for the monomer is about 37 Å, the difference of some 12 Å may indicate the extent of deformation of the monomers upon adsorption. This suggestion lends its support from the area per molecule determined, which is substantially greater than the limiting area per molecule (dimer) of some 6200 (60 × 52 × 2) Å^2, implying that a sufficient amount of space is available for structural dissociation of the dimers into monomers. As the bulk GOx concentration increased, the surface concentration also increased and the layer thickened. At 0.4 μM, the layer was 35± 2 Å thick and A reduced to some 10 000 Å^2, which is closer to the limiting value of 6200 Å^2 per dimer. The difference of some 2000 Å^2 per monomer may reflect charge related lateral repulsion. It may also be caused by a steric effect relating to NAG and MAN side chains within the adsorbed layer. The deformation of the monomers as evidenced from the variation of layer thickness may indicate that the actual empty space per monomer could

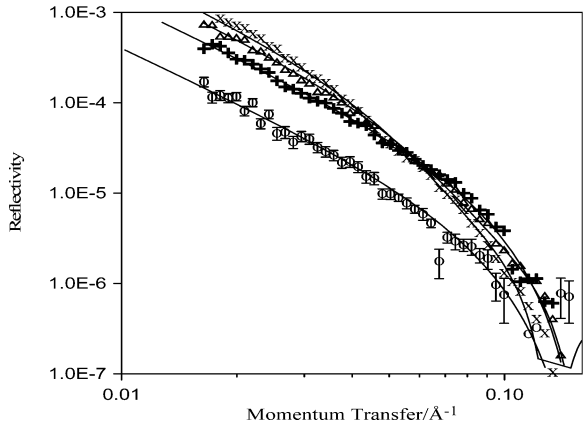

Figure 4. Neutron reflectivity measured from equilibrated GOx solution surfaces at the bulk concentrations of 0.01 (○), 0.1 (+), 0.4 (△), and 6 μM (×). For the two lower concentrations, the continuous lines represent uniform layer model fits with GOx layer thickness varying from 40 to 50 Å, indicating sideways on dimer adsorption. For the two higher concentrations, the continuous lines represent bilayer model fits, with each sublayer of 48−50 Å thick and the immersed lower layer containing 5−8% total adsorption only.

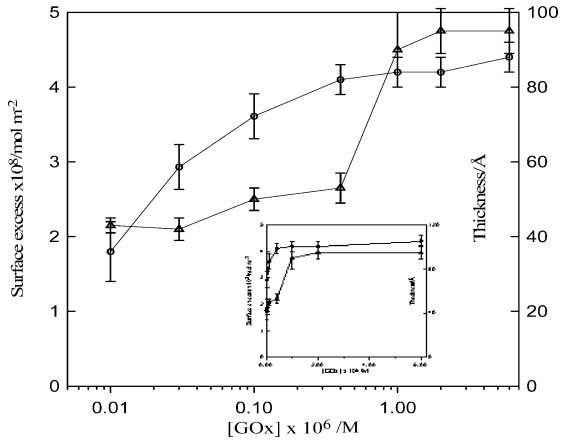

Figure 5. Variation of GOx surface excess (○) and layer thickness (+) with bulk GOx concentration. The total solution ionic strength was fixed at 0.45 M. The plots of the two parameters against the linear GOx concentration are also inserted for comparison.

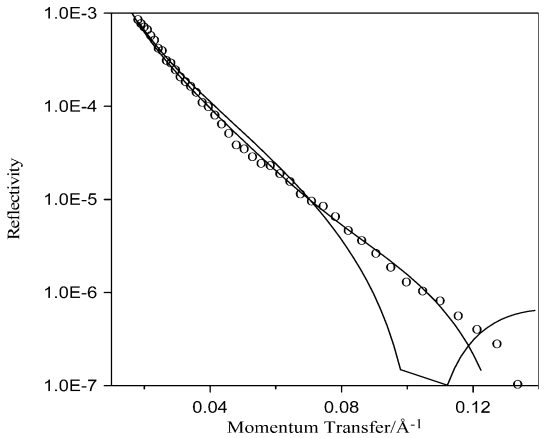

Figure 6. Comparison of a uniform layer fit of 50 Å (dashed line) with the two-layer model composed of an outer main layer on the airside and an immersed inner layer of 50 Å each (continuous line). The result clearly shows that although the amount of GOx adsorbed in the immersed layer is low, its structural distribution is easily revealed by neutron reflection. The reflectivity was measured at [GOx] = 6 mM with the total ionic strength of 0.45 M.

be much less than 2000 Å^2. This point is well supported by the measurement at the highest concentration of 1 μM. As the bulk concentration was further increased, *A* was constant at ca. 10 000 Å^2 and no longer reduced with bulk concentration. On the other hand, the layer thickness did not show much increase either. This observation indicates that while the monomers are flexible they also retain some degree of rigidity. The thickness of 37 Å at the highest GOx concentration is identical to the short axial length for the monomer. The thickness variation, together with the adsorption isotherm as shown in Figure 3, suggests that the surface adsorption tends to saturation around 0.4 μM.

C. Structural Deformation at the Higher Salt Concentration. Reflectivity measurements were also carried out at the higher ionic strength of 0.45 M and the profiles are shown in Figure 4. As in the case of the lower ionic strength, GOx adsorption initially increases fast with bulk concentration, but the gradient with increasing concentration decreases at ca. 0.1 μM and then tends to a saturation adsorption. In comparison with the reflectivity profiles shown in Figure 2, it appears that at similar GOx concentration, the level of reflectivity at the higher salt concentration was higher, indicating a trend of increasing GOx adsorption with salt addition. Moreover, while the reflectivity profiles shown in Figure 2 have relatively small variation in their shape, those in Figure 3 show a steady increase in the slope with GOx concentration. Because increased slope in the reflectivity indicates the thickening of the interfacial layer, this observation implies a relatively small change in layer thickness with increasing adsorption at the lower salt concentration, but a substantial increase in layer thickness at the higher salt concentration.

Quantitative data analysis based on the optical matrix formula produced calculated reflectivity profiles shown as continuous lines in Figure 4. The surface excess and layer thickness simultaneously determined from the data analysis are shown in Figure 5. The main observation here is the formation of uniform layer distributions up to 0.4 μM. With bulk GOx concentration above this, an adsorption bilayer formed with the secondary layer immersed in the subphase. The structural parameters obtained at the higher salt concentration suggest the retention of the GOx globular framework. There was no sign of dissociation of the dimer into monomers. Thus, below 0.03 μM, the layer was 40−45 Å thick and the area per molecule varied between some 19 000 Å^2 and 11 000 Å^2. As the bulk GOx concentration approached 0.1 μM, the layer thickness slightly increased to 50 Å, close to the short axial length of 52 Å for the nonassociated dimer. The area per molecule was found to be 9200 Å^2, as compared with the limiting area of 4620 Å^2 (60 Å × 77 Å). There is again a difference of some 4000 Å^2 between the measured limiting area and the theoretically calculated value, just as at the lower salt concentration.

Further increase in bulk GOx concentration above 1 μM resulted in the formation of a sublayer immersed in the aqueous phase underneath the main layer. Model analysis showed that both layers were about 50 Å thick and that the top layer, on the airside of the interface, contained some 90−95% of the adsorbed material. Because the composition of both layers varied little with bulk GOx concentration, the trend of further increase in the total surface excess over this high GOx concentration range was relatively small. There was no sign of unfolding of the globular framework to form polypeptide adsorption layers similar to the layers formed upon adsorption of synthetic polymers such as poly(ethylene oxide) (PEO).[26] It is important to note that although the amount of material in the sublayer was small, its presence was sensitively detected by the reflectivity measurement. Figure 6 shows the comparison of the fitting

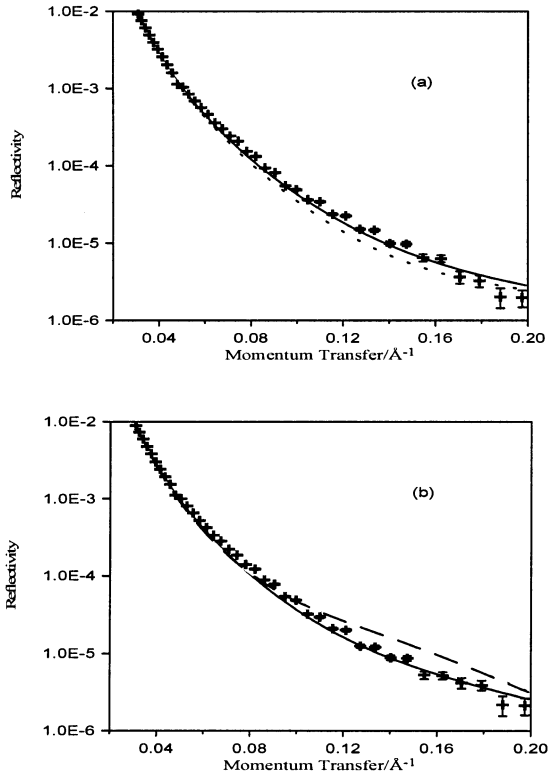

Figure 7. Neutron reflectivity profiles measured in D_2O at [GOx] = 0.01 μM, but with the ionic strength fixed at 4.5 mM (a) and at 0.45 M (b). The continuous line in panel a indicates the fitting with 3 Å of the layer staying out in the air, while the dashed line assumes some 20 Å of the layer staying out in the air. In panel b the continuous line assumes that out of the total thickness of 43 Å some 15 Å stays in the air. This is compared with the assumptions of 3 Å staying out in the air (dashed line). All other parameters used in the data analysis were taken the same as from NRW.

with and without the sublayer, and the difference clearly shows that neutron reflectivity measurement is sensitive to the thickening and inhomogeneous distribution of the GOx layer.

D. The Extent of GOx Immersion in Water. Measurements made in pure D_2O as the subphase provide information about the extent of mixing between the GOx layer and water. Under this isotopic contrast, the scattering length density of water is nonzero, and both the GOx layer and water will thus contribute to the neutron signal. Because the results shown in Figures 2 and 4 suggest different surface affinities between the monomer and dimer, neutron reflectivity measurements have been done at both salt concentrations. Figure 7 shows the best fits to the reflectivity profiles measured at [GOx] = 0.01 μM, with the ionic strength at 4.5 mM (Figure 7a) and 0.45 M (Figure 7b).

There is no substantial difference in the two reflectivity profiles shown in Figure 7. This is because a large fraction of signal arises from the air/D_2O interface. However, the structure of the GOx layer in terms of its thickness and composition and the extent of mixing of the layer will also affect the signal. At each fixed ionic strength and GOx concentration, the total layer thickness and surface excess have already been determined under NRW, as described previously. Because these parameters are the same under D_2O, the relative location of the GOx layer with respect to the surface of water can therefore be derived with reasonable confidence from the D_2O profiles.

The mixing of D_2O with the lower part of the GOx layer makes its scattering length density distinctly different from the upper part of the layer in the air. Thus, with D_2O as subphase, the GOx layer may be represented by two sublayers, the upper part of the layer in the air and the lower part of the layer immersed in water. The model and its related method of analysis are detailed in the Experimental Section.

The best fit, shown as the continuous line in Figure 7a, was calculated by taking an upper sublayer of 3−5 Å in the air and the lower sublayer of 20−22 Å immersed in water. The total layer thickness was kept the same as that determined in NRW, and the same GOx volume fraction was used in working out the respective scattering length densities. The dashed line shown in Figure 7a was calculated assuming that the layer is predominantly out of water, with 22 Å in the air and 3 Å associated with the water substrate. The poor fit in this case adds some confidence to the physical implication drawn from the measurement.

In contrast, the continuous line shown in Figure 7b was calculated assuming that the upper sublayer in the air is 15 Å and the lower sublayer in the water is 28 Å, with a total layer thickness of 43 Å. The best fit is contrasted to the poor fit representing the extreme situations of either full immersion or full floating of the GOx layer at the interface. These results thus show that monomers and dimers have different extent of immersion into water.

Discussion

The time-dependent effect detected by neutron reflection (Figure 1) is in broad agreement with results from other techniques. Neutron reflection additionally reveals changes in layer thickness and composition, from which structural deformation can be assessed. The neutron measurements at the lower salt concentration show that GOx dissociates to form monomers which adsorb with their short axial length perpendicular to the water surface. Structural changes related to the dissociation of dimers into monomers occur rather slowly: over a period of hours. The fitting of all reflectivity profiles to a single uniform layer indicates that the dissociated monomers retain their globular framework and these do not unfold further into polypeptides. Otherwise, the surface layers would be characterized by an inhomogeneous density distribution along the surface normal.[25,26] Any such inhomogeneous distribution would be more easily detected from the profiles measured in D_2O, but it was not found at both salt concentrations studied.

Hecht et al.[16] have shown that the contacts at the interface between the two monomers in the dimer are confined to a long, narrow stretch. Of these contacts, 120 are shorter than 4.0 Å, and 54 are shorter than 3.6 Å. All of these contacts are centered around 11 residues, which either form strong hydrogen bonds or salt bridges and which provide the dominant forces for dimer formation. The arrangement of the lid formed by residues 75−98 in the dimer interface effectively couples the dimer formation with the FAD binding. This segment covers the FAD binding channel in the monomer and would have to be removed before FAD could be released. This proposed change in structural conformation is broadly consistent with the FAD binding work carried out by Snoboda et al.,[27] which indicated that FAD binding involved a major conformational change. Tsuge et al.[28] showed that the apoenzyme, later shown to be the monomers, was more susceptible to proteolysis. They speculated that before binding FAD the lid is in an open conformation. Upon binding the lid returns to the closed conformation, forms the dimer interface, and encloses the FAD moiety. Thus, the dissociation of dimers into monomers involves structural changes coupled with breaking of hydrogen bonds and salt bridges.

The data shown in Figures 3 and 5 suggest that the variation of surface excess with bulk concentration was different for the

two salt concentrations. Although the surface excess obtained at the higher salt concentration was overall greater than at the lower salt concentration, the surface excess values determined over the lowest GOx concentration range were similar. This observation may suggest that at the low GOx concentration dissociated monomers are as surface active as nondissociated dimers. However, as the bulk concentration increased, the dimers were clearly more surface-active and reached saturation adsorption at the lower GOx concentration of 0.1 μM. In contrast, the saturation point for the dissociated monomers was around 0.4 μM. The difference is not unexpected. The dimers and the dissociated monomers do not have to show the same surface activity. Indeed, the monomers and dimers may effectively be regarded as different species because of their different sizes and different surface peptide distributions.

Rinuy et al. have studied the adsorption of GOx at the air/water interface using second harmonic generation (SHG). The experimental signal arises from the absorption of the chromophoric group corresponding to the $\pi-\pi^*$ transitions along the three cycles of the isoalloxazine ring in the FAD structure. Their measurement of GOx adsorption at pH 7 and at a total ionic strength of 0.1 M shows a progressive increase in SHG signal (the square root of which is proportional to surface excess) up to about 0.3 μM, in broad agreement with our neutron data obtained at the higher total buffer concentration. At the higher GOx concentration, the SHG signal declined, and the authors suggested that the change indicated interfacial structural reorganization. It is, however, difficult to infer the structural details from the SHG data. Nevertheless, the broad trend of the structural reorientation detected from the SHG experiment is entirely consistent with the bilayer formation unravelled from neutron reflection. It is also interesting to add that because SHG is sensitive to the presence of FAD groups and their structural environment at the interface, it would be useful to apply SHG to detect the possible dissociation of FAD groups from the monomers that we have shown to be the adsorbed species with lower ionic strength of the aqueous phase.

The difference in surface excess obtained as shown in Figures 3 and 5 correlates with the change in the extent of electrostatic repulsion within the adsorbed layer and the degree of hydration of the protein molecule itself. It appears that the smaller the electrostatic repulsion, the bigger the surface excess. An increase of the net charges of the enzyme also increases its hydrophilicity, which would reduce the tendency to adsorb at a hydrophobic surface such as air. Salt addition reduces the difference between the surface excesses obtained from different concentrations higher than 0.4 μM. At high salt concentration the electrostatic charges on the protein are screened, which would favor increase of the overall level of adsorption. It is relevant to note that Rosilio et al. also noted, from surface potential measurement, a structural "anomaly" for the GOx concentrations over 0.2 μM. Again, like many other techniques, the surface potential study could not decipher the structural mystery.

The adsorption isotherms are broadly similar to those obtained for globular proteins such as lysozyme and HSA (human serum albumin),[30,31] but for these compact proteins, the limiting area per molecule is, within the experimental error, close to the values estimated from the dimensions of crystalline structures. Thus, for lysozyme, *A* was found to be some 950 Å and equal to that (30 Å $\times$ 30 Å) estimated from the solution crystalline structure at the saturated monolayer adsorption. This value of *A* is consistent with the thickness of 45−47 Å simultaneously determined, indicating a headways-on lysozyme layer formation at pH 7. In comparison, HSA and BSA form sideways-on monolayers. For these proteins, and as the adsorption approaches the formation of saturated monolayers, the layer thickness gradually increases and eventually becomes comparable to the short axial dimension (40 Å) of the crystalline structure. Over the saturated monolayer region, *A* is also comparable to the limiting area per molecule estimated from the three-dimensional structure. The main similarity between the albumins and GOx is the gradual thickness increase, indicative of structural deformation within the monolayers. However, for GOx, we have shown that at both salt concentrations, the *A* at the saturated monolayer adsorption is 3000−4000 Å^2 greater than the values estimated from the appropriate dimensions of crystalline structure. This apparent discrepancy may arise from electrostatic repulsion within the layer and the steric effect relating to the side chain carbohydrate groups.

It is customary to assume that the monolayer formed by globular proteins at the air/water interface is fully immersed in water (e.g, the work by Wang et al.[32]). However, our recent neutron reflection data shows that this is not always so [see ref 30a]. The current neutron work shows that while the dissociated monomers are rather immersed in water, the nondissociated dimers are only partially immersed. The binding interface contains many polar and charged groups and their burial in the dimer is expected to increase the protein surface hydrophobicity for the dimer. Our deduction of an adsorption at the interface greater for the dimers than for the monomers is consistent with this assumption. Furthermore, dimer formation and dissociation involve three-dimensional structure changes. The partial immersion of the dimers may be caused by the distribution of the carbohydrate side chains that promote the surface hydrophobic effect. The higher immersion of the monomers may be caused partly by the exposed binding interface after dissociation and partly by the distribution of hydrophobic and nonpolar groups which may not favor exposure on to the surface. The current experiment lacks of local structural resolution and so was unable to identify the regions that are out of water.

Conclusions

We have shown that the high depth resolution of neutron reflection is capable of quantitative determination of interfacial structure and composition for protein layers. The GOx work demonstrates the formation of interfacial layers with uniform density distributions, indicating that despite dissociation and deformation no further structural deterioration occurs. The structural information for the interfacial layers, together with the known three-dimensional structures of proteins, allows a systematic assessment of structural deformation and possible unfolding caused by either surface specific effects or solution conditions.

The main finding from this work, as outlined in the schematic diagram in Figure 8, shows the dissociation of the GOx dimer into adsorbed monomers at lower solution ionic strength and the retention of the globular dimer framework in the adsorbed layer at the higher salt concentration. Both monomers and dimers show structural deformation upon adsorption (not represented in Figure 8), the extent of which can be assessed from the relative variation of layer thickness under monolayer adsorption. Both monomers and dimers are adsorbed sideways-on, with their long axis projected in parallel with the solution surface. The different shape of adsorption isotherms at different ionic strength is consistent with the different extent of layer immersion into water for the monomer and dimer, indicating different surface adsorption properties of the two species, consistent with the nature of the amino acids exposed on the protein exterior in

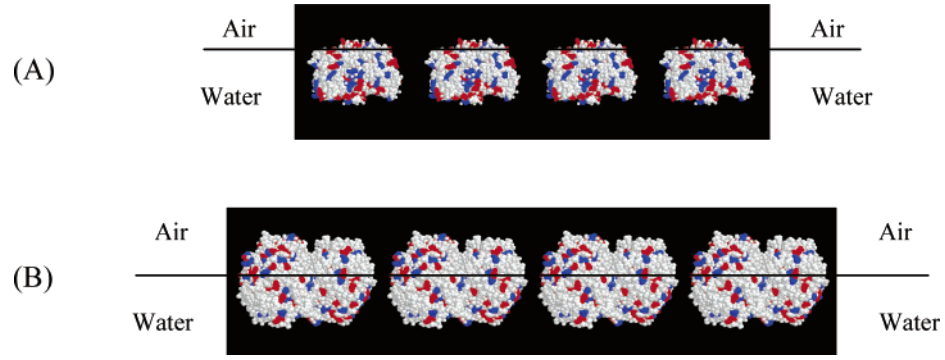

Figure 8. Schematic representation of GOx structural conformations on the surface of water: (A) monomer adsorption at low salt concentration and (B) dimer adsorption at high salt concentration. The lines indicate the air/water interface.

the two species. The formation at the higher salt concentration of a secondary layer immersed in the subphase underneath the main outer layer (not shown in Figure 8) did not cause a substantial increase in the total surface excess because the amount of material deposited in the secondary layer was only some 5−8% of the total. Nevertheless, the presence of this layer caused substantial changes to the shape of neutron reflectivity profiles, indicating the high sensitivity of this technique to the volume fraction distribution of protein layers across the interface.

A wide range of technological applications of proteins and enzymes is based on their behavior at the solid/water interface. We have recently demonstrated that the neutron reflection experiment can also provide valuable information about structural features relating to the interfacial responses of globular proteins such as lysozyme, BSA and HSA.[13−15] Glycoproteins such as GOx have more elaborate three-dimensional structures, and the evolution of structural details at interfaces can be complicated by various factors. The use of the air/water interface in this work serves as a model so that further effects arising from surface chemistry as in the case of solid/solution interface can be subsequently assessed. This technical advantage makes it feasible to detect structural unfolding of a range of proteins across model cell membranes and to relate the molecular structures of enzymes to their bioactivities.

Experimental Section

Neutron reflection measurements were performed on the white beam reflectometer SURF at the Rutherford Appleton Laboratory, ISIS, Didcot, U.K., using neutron wavelengths from 0.5 to 6.5 Å. The aqueous solutions were poured into Teflon troughs to give a positive meniscus to prevent obstruction of the incoming and reflected beam by the Teflon. The troughs were mounted on an antivibration table with five trough slots, which allowed the continuous monitoring of the reflectivity of the sample until a steady value was obtained. The alignment of each trough was established by adjusting each time the appropriate heights using a laser beam that shared the same beam path as the neutron beam. The collimated neutron beam was reflected at the air/liquid interface at three different glancing angles, 1.5°, 0.8 °, and 0.5 °, and the three reflectivity curves were subsequently merged manually to produce a κ range necessary to determine the layer thickness, with appropriate scaling factors. The beam intensity was calibrated with respect to clean D_2O. A flat background was determined by extrapolation to high values of κ. All the experiments were carried out at 25 °C.

Glucose oxidase was purchased from Sigma (type VII-S from *Aspergillus niger*, Cat. No G7016) and was used as supplied throughout the experiment. GOx consists of 20 different amino acids of a known sequence[22] and a redox coenzyme, flavin adenine dinucleotide, per monomer that is not covalently bound to the protein and can be released under denaturing conditions. The native protein is acidic with an isoelectric point of 4.44, and at pH 7 it is negatively charged, with 11 charges and a negative ζ potential around −14 mV. GOx has several hydrophobic side-chains located near the surface of the GOx globule. This hydrophobic surface is thought to be the driving force for spontaneous adsorption at the air/water interface. The GOx solutions were all made up using Elgastat ultrapure (UHQ) water in phosphate buffer of two different ionic strengths 0.45 M and 4.5 mM, with pH adjusted to 7 by using a respective 1:1 ratio of K_2HPO_4 and $KH_2PO_4 \cdot 3H_2O$. All glassware and the Teflon troughs were thoroughly cleaned with an alkaline detergent (Deacon 90) and repeatedly rinsed with UHQ water.

Neutron Reflection

Neutron reflectivity, $R(\kappa)$, was measured as a function of momentum transfer, κ, perpendicular to the reflecting surface. $R(\kappa)$ is related to the scattering length density perpendicular to the interfacial plane, $\rho(z)$, by

$$R(\kappa) = \frac{16\pi^2}{\kappa^2}|\hat{\rho}(\kappa)|^2 \tag{4}$$

$$\hat{\rho}(\kappa) = \int_{-\infty}^{\infty} \exp(-i\kappa z)\rho(z)\, dz \tag{5}$$

where the scattering length density depends on chemical composition through the following equation:

$$\rho = \sum n_i b_i \tag{6}$$

where n_i is the number density of the element, i, and b_i is its scattering density. Because different isotopes have different b_i values, by the use of isotopic substitution, a variety of neutron reflection profiles can be produced for a given chemical structure. The NRW water and D_2O were used in this work to highlight the GOx layers differently.

Although the principal relationship between R(κ) and ρ outlined in eqs 6−8 is very straightforward, neutron reflectivity profiles are usually analyzed by means of the optical matrix formalism, which has been described in detail elsewhere.[33] The main difficulty in Fourier transforming these reflectivity profiles is that the data were measured over too narrow a κ range to allow for a reliable determination of phases. A typical modeling procedure is usually started with an assumption of a structural model for the adsorbed layer, followed by calculation of the reflectivity based on the optical matrix formula. The calculated reflectivity is then compared with the measured data. In a more

general situation where the adsorbed protein layer is partially immersed in water, the upper part of the layer is out in air, and the lower part of the layer is predominantly immersed in water. This uneven water distribution can be approximated to a two layer model when D_2O is used, with the upper part of the layer completely dry and lower layer fully immersed in water. Although eqs 2−4 have been developed under the condition of uniform layer distribution, they are directly applicable to each of the sublayers when more than one layer is required to model the density distribution profiles. The choice of the number of sublayers is dependent upon the extent of inhomogeneity across the interface. However, in general the minimum number of layers that will successfully fit the data is chosen.

The calculation of structural parameters requires the total scattering length whose value was obtained from the primary sequence of the enzyme. This information can be accessed from the Brookhaven Protein Data Bank.[22] Because GOx contains labile hydrogens on the main peptide chains and the amino acid side groups, which readily exchange with D_2O, due consideration should be taken into the effect of H/D exchanges on the scattering length. It has been suggested that tight globular structure associated with hydrophobic encapsulation and hydrogen bonding could inhibit the dynamic processes of H/D exchanges.[23,24] However, our previous work has indicated that even for more robust globular proteins such as lysozyme and albumins, interfacial adsorption related to the structural deformation resulted in almost complete exchange.[13,14] Because GOx is a much larger but less stable protein, we have assumed that the H/D exchange was complete during the course of surface adsorption. The resulting values of scattering length were calculated to be 0.32 Å in NRW and 0.51 Å in D_2O. The contributions from five *N*-acetyl-d-glucosamine groups (NAG), three α-D-mannose groups (MAN), and one flavin adenine dinucleotide (FAD) on each monomer and their labile hydrogen exchanges have also been taken into account. It is obvious that any error in this assumption would affect the value in D_2O but has little effect on the value in NRW. The molecular volume for GOx was estimated to be 1.45×10^5 Å^3 by adding the volumes of all the peptide chains and the carbohydrate moieties. The scattering length densities were calculated to be 2.2×10^{-6} Å^{-2} in NRW and 3.5×10^{-6} Å^{-2} in D_2O. The accuracy of these values is dependent on the assumption of compete H/D exchange and the estimate of molecular volume, but it is reassuming to find that within $\pm 0.1 \times 10^{-6}$ Å^{-2} these values are identical to those for lysozyme and HSA (human serum albumin).[13]

The determination of the extension of the protein layer into air was made using D_2O as subphase. The GOx layer was represented by two sublayers, the upper part of the layer in the air and the lower part of the layer immersed in water. For the upper sublayer, eqs 2 and 3 still apply. The fraction of the scattering length for the upper sublayer is proportional to its thickness (τ_1). For the sublayer under the water, eq 2 needs to be modified to take into account the contribution of scattering length from the water (b_w):

$$\rho_2 = \frac{(1-f)\sum m_p b_p + n b_w}{A\tau_2} \tag{7}$$

where n is the number of water associated with each protein molecule, f is the fraction of the GOx layer floating out of water, and ρ_2 and τ_2 are the scattering length density and thickness for the lower sublayer. Although ρ_1 and ρ_2 can be obtained from eqs 2 and 4, the more direct approach is through the following equation:

$$\rho_i = \phi_p \rho_p + \phi_{iw} \rho_w \tag{8}$$

where ρ_p and ρ_w are the scattering length densities of protein and water and ϕ_p and ϕ_{iw} their respective volume fractions. For the upper sublayer, $i = 1$, $\phi_{1w} = 0$. For the lower sublayer, $i = 2$, $\phi_{2w} = 1 - \phi_p$. Thus, for adsorption at a given GOx concentration and ionic strength, ρ_1 and ρ_2 are fixed and the only parameters that can be varied are τ_1 and τ_2. Because of H/D exchanges, ρ_p and ρ_w in D_2O are greater than their corresponding values in NRW. As already explained, the extent of H/D exchanges was taken to be complete.

Acknowledgment. This work was supported by the Biotechnology and Biological Sciences Research Council (BBSRC), the Engineering and Physical Sciences Research Council (EPSRC), and the TMR Program of the European Union (Project FMRX-CT96-0078).

References and Notes

(1) MacPhee, C. E.; Dobson, C. M. *J. Am. Chem. Soc.* **2000**, *122*, 12707−12713.
(2) Chiti, F.; Bucciantini, M.; Capanni, C.; Taddei, N.; Dobson, C. M.; Stefani, M. *Protein Sci.* **2001**, *10*, 2541−2547.
(3) Fandrich, M.; Fletcher, M. A.; Dobson, C. M. *Nature* **2001**, *410*, 165−166.
(4) Moussy, F.; Harrison, D. J.; O'Brien, D. W.; Rajotte, R. V. *Anal. Chem.* **1993**, *65*, 2072−2077.
(5) Linke, B.; Kerner, W.; Kiwit, M.; Pishko, M.; Heller, A. *Biosens. Bioelectron.* **1994**, *9*, 151−158.
(6) Abel, P. U.; von Woedtke, Th.; Schulz, B.; Bergann, Th.; Schwock, A. *J. Mol. Catal. B: Enzymatic* **1999**, *7*, 93−100.
(7) Zhang, J.; Rosilio, V.; Goldmann, M.; Boissonnade, M. M.; Baszkin, A. *Langmuir* **2000**, *16*, 1226−1232.
(8) Tripp, B. C.; Magda, J. J.; Andrade, J. D. *J. Colloid Interface Sci.* **1995**, *173*, 16−27.
(9) Xu, S.; Damodaran, S. *Langmuir* **1994**, *10*, 472−480.
(10) Rapoza, R. J.; Horbett, T. A. *J. Colloid Interface Sci.* **1990**, *136*, 480−493.
(11) Rinuy, J.; Brevet, P. F.; Girault, H. H. *Biophys. J.* **1999**, *77*, 3350−3355.
(12) Fragneto, G.; Thomas, R. K.; Rennie, A. R.; Penfold, J. *Science* **1995**, *267*, 657−660.
(13) (a)Su, T. J.; Lu, J. R.; Thomas, R. K.; Cui, Z. F. *J. Phys. Chem. B* **1999**, *103*, 3727−3736. (b) Su, T. J.; Lu, J. R.; Thomas, R. K.; Cui, Z. F.; Penfold, J. *Langmuir* **1998**, *14*, 438−445.
(14) (a) Lu, J. R.; Su, T. J.; Thomas, R. K.; Penfold, J. *Langmuir* **1998**, *14*, 6261−6268. (b) Lu, J. R.; Su, T. J.; Thomas, J. *J. Phys. Chem. B* **1998**, *102*, 10307−10315.
(15) (a) Green, R. J.; Su, T. J.; Lu, J. R.; Webster, J. R. P. *J. Phys. Chem. B* **2001**, *105*, 9331−9338. (b) Green, R. J.; Su, T. J.; Lu, J. R.; Penfold, J. *J. Phys. Chem. B* **2001**, *105*, 1594−1602.
(16) (a) Hecht, H. J.; Kalizs, H. M.; Hendle, J.; Schmid, R. D.; Schomburg, D. *J. Mol. Biol.* **1993**, *229*, 153−172. (b) Hecht, H. J.; Schomburg, D.; Kalizs, H. M.; Schmid, R. D. *Biosens. Bioelectronics.* **1993**, *8*, 197−203.
(17) Sun, S. C.; Ho−Si, P. H.; Harrison D. J. *Langmuir* **1991**, *7*, 727−737.
(18) Fiol, C.; Valleton, J. M.; Delphire, N.; Barbey, D.; Barraud, A.; Ruaudel-Teixier, A. *Thin Solid Films* **1992**, *210*, 489−491.
(19) Bazskin, A.; Boissonnade, M. M.; Rosilio, V.; Kamyshny, A.; Magdassi, S. *J. Colloid Interface Sci.* **1997**, *190*, 313−317.
(20) Lu, J. R.; Thomas, R. K. *J. Chem. Soc., Faraday Trans.* **1998**, *94*, 995−1018.
(21) Lu, J. R.; Lee, E. M.; Thomas, R. K. *Acta Crystallogr., Sect. A* **1996**, *52*, 11−41.
(22) Wohlfahrt, G.; Witt, S.; Hendle, J.; Schomburg, D.; Kalisz, H. M.; Hecht, H. J. *Acta Crystallogr., Sect. D* **1999**, *55*, 969. (b) Kriechbaum, M.; Heilmann, H. J.; Wientjes, F. J.; Hahn, M.; Jany, K.-D.; Gassen, H. G.; Sharif, F.; Alaeddinoglu, G. *FEBS Lett.* **1989**, *255*, 63−66.
(23) Hvidt, A.; Nielsen, S. O. *Adv. Protein Chem.* **1966**, *21*, 287−310.
(24) Radford, S. E.; Buck, M.; Topping, K. D.; Dobson, C. M.; Evans, P. A. *Proteins: Struct. Func. Genet.* **1992**, *14*, 237−248.

(25) Lu, J. R.; Su, T. J.; Thomas, R. K.; Rennie, A. R.; Cubit, R. *J. Colloid Interface Sci.* **1998**, *206*, 212−223.
(26) Lu, J. R.; Thomas, R. K.; Penfold, J.; Richards, R. W. *Polymer* **1996**, *37*, 109−114.
(27) (a) Snowboda, B. E. P. *Biochim. Biophys. Acta* **1969**, *175*, 365−379. (b) Snowboda, B. E. P. *Biochim. Biophys. Acta* **1969**, *175*, 380−387.
(28) Tsuge, H.; Natsuaki, O.; Ohashi, K. *J. Biochem.* **1975**, *78*, 835−843.
(29) Rosilio, V.; Boissonnade, M.-M.; Zhang, J.; Jiang L.; Bazskin, A. *Langmuir* **1997**, *13*, 4669−4675.
(30) Lu, J. R.; Su, T. J.; Thomas, R. K.; Penfold, J.; Webster, J. *J. Chem. Soc. Faraday Trans.* **1998**, *94*, 3279−3287.
(31) Lu, J. R.; Su, T. J.; Penfold, J. *Langmuir* **1999**, *15*, 6975−6983.
(32) Wang, J.; McGuire, J. *J. Colloid interface Sci.* **1997**, *185*, 317−323.
(33) Born, M.; Wolf, E. *Principles of Optics*; Pergamon: Oxford, 1970.